

**Regularization of chaos by noise in electrically driven nanowire systems**Peyman Hessari,<sup>1,\*</sup> Younghae Do,<sup>2,†</sup> Ying-Cheng Lai,<sup>3,4</sup> Junseok Chae,<sup>3</sup> Cheol Woo Park,<sup>1</sup> and GyuWon Lee<sup>5</sup><sup>1</sup>*School of Mechanical Engineering, Kyungpook National University, Daegu, 702-701, Korea*<sup>2</sup>*Department of Mathematics, KNU-center for Nonlinear Dynamics, Kyungpook National University, Daegu, 702-701, Korea*<sup>3</sup>*School of Electrical, Computer and Energy Engineering, Arizona State University, Tempe, AZ 85287, USA*<sup>4</sup>*Department of Physics, Arizona State University, Tempe, Arizona 85287, USA*<sup>5</sup>*Department of Astronomy and Atmospheric Sciences, Center for Atmospheric Remote Sensing(CARE), Kyungpook National University, Daegu, 702-701, Korea*

(Received 12 October 2013; revised manuscript received 1 March 2014; published 8 April 2014)

The electrically driven nanowire systems are of great importance to nanoscience and engineering. Due to strong nonlinearity, chaos can arise, but in many applications it is desirable to suppress chaos. The intrinsically high-dimensional nature of the system prevents application of the conventional method of controlling chaos. Remarkably, we find that the phenomenon of coherence resonance, which has been well documented but for low-dimensional chaotic systems, can occur in the nanowire system that mathematically is described by two coupled nonlinear partial differential equations, subject to periodic driving and noise. Especially, we find that, when the nanowire is in either the weakly chaotic or the extensively chaotic regime, an optimal level of noise can significantly enhance the regularity of the oscillations. This result is robust because it holds regardless of whether noise is white or colored, and of whether the stochastic drivings in the two independent directions transverse to the nanowire are correlated or independent of each other. Noise can thus regularize chaotic oscillations through the mechanism of coherence resonance in the nanowire system. More generally, we posit that noise can provide a practical way to harness chaos in nanoscale systems.

DOI: [10.1103/PhysRevB.89.134304](https://doi.org/10.1103/PhysRevB.89.134304)

PACS number(s): 05.45.Xt, 05.45.Pq, 85.85.+j

**I. INTRODUCTION**

Nanoelectromechanical (NEM) systems are at the frontier of nanoscience and nanotechnology. Their small size, extremely low power consumption, and ultrafast operational speed are among the virtues that have been exploited for significant applications ranging from single-electron spin detection [1] and Zeptogram scale mass sensing [2] to rf communications [3], semiconductor superlattice [4,5], and many others [6–14]. From the perspective of basic science, NEM systems represent a novel class of high-dimensional nonlinear dynamical systems. Recent years have witnessed a growing interest in exploring and understanding various nonlinear phenomena in NEM systems such as synchronization [15], signal amplification and stochastic resonance [16,17], extensive chaos [18], and multistability [19].

To see why NEM systems are fundamentally nonlinear and thus chaos can arise, we take as an example an electrostatically driven nanowire [1,2,8,9,12–14,20–22], a paradigm for investigating nonlinear behaviors in nanoscale systems [15,18,19]. When the nanowire moves, the amount of stretching can be expressed as an integral of nonlinear functions of the displacements (see Sec. II below). In addition, the electrical force on the wire depends on its displacement in a nonlinear fashion. Chaotic motions can thus be anticipated. In fact, both small-scale, localized chaotic attractors and large-scale, extensive chaos have been uncovered in the Si-nanowire system [18]. While chaos, especially extensive chaos, can be exploited for applications such as ultrafast (GHz range)

random-number generators [18], there are applications that require regular oscillations of the nanowire, where chaos is undesirable. In principle, chaos can be controlled by using small, judiciously chosen perturbations [23], but this is effective mostly for low-dimensional dynamical systems [24]. Due to the high-dimensional nature and their small physical sizes, nanowire systems may not be susceptible to the conventionally available methods of chaos control. It is necessary to develop alternative, experimentally feasible approach to suppressing chaos in nanoscale systems.

In this paper, we articulate and demonstrate an experimentally viable approach to harnessing chaos in electrostatically driven nanowire systems. The idea is to make use of stochastic driving or noise. In particular, the interplay between nonlinearity and stochasticity can lead to interesting phenomenon such as stochastic resonance [25–30], where a suitable amount of noise can counter-intuitively optimize the characteristics of the system output such as the signal-to-noise ratio. Previous works also uncovered the remarkable phenomenon of noise-induced frequency [31] or coherence resonance [32–34] where, when a nonlinear oscillator is under stochastic driving, a dominant Fourier frequency in its oscillations can emerge, resulting in a signal that can be much more temporarily regular than that without noise [31–34]. A closely related phenomenon is noise-induced collective oscillation or stochastic resonance in the absence of an external periodic driving in excitable dynamical systems [35]. Quantitatively, associated with coherence resonance, the temporal regularity of the system dynamics depends on the noise amplitude and it can be maximized by noise of optimal amplitude. There were extensive studies of coherence resonance in the past decades both theoretically [36–42] and experimentally [43–45]. For low-dimensional chaotic systems, coherence resonance has also been studied [33,34,46–48].

\*Present address: Department of Mathematical Sciences, UNIST, Ulsan, 689-798, Korea.

†yhdo@knu.ac.kr

There have also been recent works on coherence resonance in nanoscale systems [49–51]. In particular, coherence resonance in a single-walled Carbon nanotube ion channel was uncovered [49]. It was found [50] that the regularity of the spatial distribution of pores in a nanostructure can be maximized by some optimal level of internal noise. It was also discovered [51] that the electron dynamics in a semiconductor superlattice can exhibit coherence resonance. In these works, the intrinsic dynamics of the nanoscale systems were regular, and the systems were assumed to be in low-temperature environment. In our work, the underlying nanoscale system is silicon nanowire, which mathematically is described by a set of two coupled nonlinear partial differential equations (PDEs), subject to external driving and noise. The simulation and analysis of our system is thus significantly more challenging than those for systems described by ordinary differential equations (ODEs). Physically, as compared with the existing works in Refs. [49–51], the distinct features of our present work are twofold: (1) we study the parameter regime where the deterministic dynamics are chaotic and motivate our work from the perspective of control, and (2) we assume that the operational environment of the nanowire is under room conditions. The issue of chaos control is challenging, as existing methods cannot be extended to the nanowire system.

Our main result is that, when the nanowire system is driven to chaos, noise can make the oscillations much more regular. Specifically, we find that, because of chaos, the oscillations of the wire are highly irregular in the deterministic case, but the wire can oscillate much more regularly when the noise amplitude is in the vicinity of some optimal value. This is unequivocal evidence of coherence resonance in the nanowire system *even when it is in chaotic regime*. We also find that coherence resonance in the nanowire system is robust because it occurs regardless of whether noise is white or colored, and of whether the stochastic drivings in the two independent directions transverse to the nanowire are correlated or independent of each other. Because of the feasibility in applying noise to a nanowire system, e.g., by controlling the temperature of the surroundings, we expect that our idea of exploiting noise to regularize chaos in nanoscale systems to be experimentally verifiable and practically implementable.

## II. MODEL AND METHODS

Figure 1 shows the device configuration of a suspended nanowire [14] in an environment of random thermal fluctuations. It is a solid structure with two ends bridging the sidewalls. When driven externally by a relatively weak force, the nanowire oscillates vertically in the  $z$  direction as a doubly clamped beam. However, when the force is sufficiently large to yield substantial bending and consequently generate strong axial stress, the planar vibration is no longer stable and the wire can bend to its sides ( $y$  direction) and rotate in the  $y$ - $z$  plane. As the magnitude of the driving force is increased further, small-scale chaotic motions and then extensive chaos can occur [18]. Intuitively, one would expect the motion of the wire to be random in the chaotic regime, especially when noise is present.

A dynamical analysis of the driven nanowire system subject to periodic electrical driving and noise requires combined solutions of the mechanical, electrical, and molecular-interaction

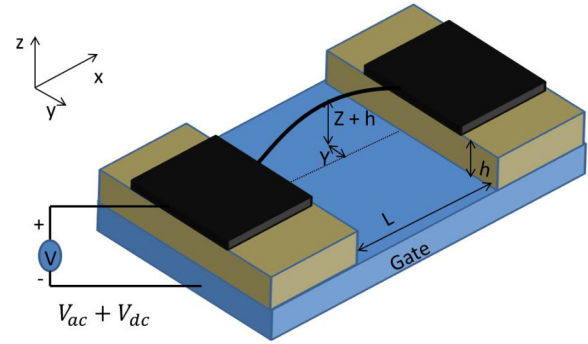


FIG. 1. (Color online) Schematic illustration of an electrostatically driven, suspended nanowire of length  $L$  and diameter  $d$ .

(fluid) equations governing the motion of the wire. In the following, we briefly describe the main ingredients of the model.

*Mechanical equations.* We consider a nanowire of constant, circular cross-sectional area  $A$  (radius  $r$ ) and apply the standard Euler-Bernoulli theory to obtain [14] the following set of PDEs governing the displacements  $Z(x, t)$  and  $Y(x, t)$  of the wire in the  $z$  and  $y$  directions, respectively:

$$\begin{aligned} \rho A Z_{tt} + EI Z_{xxxx} - \frac{EA}{2L} Z_{xx} \int_0^L (Y_x^2 + Z_x^2) dx &= F_e(Z) + F_f^Z, \\ \rho A Y_{tt} + EI Y_{xxxx} - \frac{EA}{2L} Y_{xx} \int_0^L (Y_x^2 + Z_x^2) dx &= F_f^Y, \end{aligned} \quad (1)$$

where  $F_e(Z)$  is the electrical force acting on the wire in the  $z$  direction,  $F_f^Z$  and  $F_f^Y$  are the viscous damping forces in the  $z$  and  $y$  directions, respectively,  $E$  is the Young's modulus, and  $I = \pi r^4/4$  is the moment of inertia of the wire's cross-sectional area.

*Electrical force.* Let  $h$  be the vertical distance between the clamped ends of the nanowire and the surface of the substrate,  $d = 2r$  be the cross-sectional diameter of the wire, and  $V(t)$  be the external voltage applied to the wire. Under the condition  $h \gg d$  so that the oscillation amplitude is much smaller than that for the onset of the pull-in effect [8,9], the electrical force per unit length is given by [18]

$$F_e(Z) = -\frac{\pi \epsilon V^2(t)}{(Z+h) \left[ \ln \left( 4 \frac{Z+h}{d} \right) \right]^2}, \quad (2)$$

where  $\epsilon$  is the dielectric constant of the homogeneous medium in which the nanowire is immersed.

*Average molecular-interaction (fluid) force.* Due to the small scale of the wire size, under room conditions, its oscillations in a gaseous medium (e.g., air) are governed by molecular-regime physics for which the drag force on the wire is due to the momentum exchange with the surrounding gas molecules. It can be derived [18,52] that the  $z$  and  $y$  components of the total drag force acting on the nanowire per unit length are

$$F_f^Z(x, t) = \frac{\pi P d}{4v_T} Z_t(x, t), \quad F_f^Y(x, t) = \frac{\pi P d}{4v_T} Y_t(x, t), \quad (3)$$

where  $P$  and  $v_T$  are pressure and molecular velocity, respectively.

*Stochastic driving force.* We develop a physically meaningful approach to incorporating random fluctuations in the nanowire model. The fluid forces as given by Eq. (3) are *average* forces acting on the nanowire due to its interaction with the medium molecules. In physical reality, random molecular fluctuations in the fluid environment are inevitable, requiring that Eq. (3) be modified. There are two parameters in the force expressions, which characterize the physical properties of the environmental fluid: pressure  $P$  and the molecular velocity  $v_T$ . Statistical fluctuations in the molecular motion render collisions of the molecules with the nanowire surface random. As a result, the instantaneous pressure can be written as  $P(t) = \bar{P} + \varepsilon_P(T)\xi(t)$ , where  $\bar{P}$  is the average pressure,  $\varepsilon_P(T)$  is the amplitude of the pressure fluctuation that depends on the temperature  $T$ , and  $\xi(t)$  is a stochastic process of zero mean and unit variance. The molecular velocity  $v_T$  is directly proportional to  $\sqrt{T}$ . Since temperature  $T$  typically varies slowly as compared with the process of molecular collision,  $v_T$  can be regarded as a constant. Under stochastic fluctuations, Eq. (3) should thus be modified to

$$\begin{aligned} F_f^Z(x,t) &= \frac{\pi d[\bar{P} + \varepsilon_P(T)\xi(t)]}{4v_T} Z_t(x,t), \\ F_f^Y(x,t) &= \frac{\pi d[\bar{P} + \varepsilon_P(T)\xi(t)]}{4v_T} Y_t(x,t). \end{aligned} \quad (4)$$

Substituting these force expressions into Eq. (1), we obtain a pair of stochastic nonlinear PDEs governing the dynamics of the nanowire under random fluctuations. The fluctuation or noisy terms depend on the velocity components of the nanowire. Strictly speaking, the corresponding stochastic processes are not white Gaussian but are “colored” instead. Treating colored noise even for systems described by ODEs is challenging [53]. To gain insight, we initially consider the following simplified version of the electrically and randomly driven PDEs:

$$\begin{aligned} \rho A Z_{tt} + EIZ_{xxxx} - \frac{EA}{2L} Z_{xx} \int_0^L (Y_x^2 + Z_x^2) dx \\ = F_e(Z) + \bar{F}_f^Z + \varepsilon_z \eta(t), \end{aligned} \quad (5)$$

$$\begin{aligned} \rho A Y_{tt} + EIY_{xxxx} - \frac{EA}{2L} Y_{xx} \int_0^L (Y_x^2 + Z_x^2) dx \\ = \bar{F}_f^Y + \varepsilon_y \eta(t), \end{aligned} \quad (6)$$

where  $\varepsilon_z$  and  $\varepsilon_y$  are the fluctuation or noise amplitude in the  $z$  and  $y$  direction, respectively, and  $\eta(t)$  is a Gaussian random process of zero mean and unit variance. For convenience, we write  $\varepsilon_z \equiv D \sin(\theta)$  and  $\varepsilon_y \equiv D \cos(\theta)$ , where  $D$  is the noise amplitude and  $\theta$  is a random variable uniformly distributed in  $[0, 2\pi]$ .

In general, the random processes  $\xi(t)Y_t(x,t)$  and  $\xi(t)Z_t(x,t)$  in Eq. (4) are not strictly Gaussian, as  $Y_t(x,t)$  and  $Z_t(x,t)$  are deterministically chaotic with correlations. This issue can be addressed from the following two aspects. First, we calculate the statistical distributions of the two random processes for a large number of parameter configurations. In all cases, we find that the distributions of  $\xi(t)Y_t(x,t)$  and  $\xi(t)Z_t(x,t)$  decay extremely rapidly from the peaks at their

respective average values, suggesting that it is reasonable to treat the random processes as approximately Gaussian. Second, we investigate how violation of the Gaussian assumption affects the coherence resonance. Especially,  $\xi(t)Y_t(x,t)$  and  $\xi(t)Z_t(x,t)$  are generally “colored,” and we calculate the coherence-resonance measure for colored noise (to be shown). We find that the chaotically oscillating nanowire exhibits qualitatively and quantitatively similar coherence resonance for Gaussian and colored noise, providing justification to treat the noise fluctuations in the nanowire as Gaussian.

*Numerical procedure for solving the electrically and stochastically driven nanowire system.* We use the standard finite-element (FE) method to solve the nanowire equations [19]. The basic steps are: discretization, choosing approximation model and base functions, deriving element equations using the weighted residue method, assembling these equations to obtain a global matrix representation, and solving a set of initial value problems under stochastic forcing. For *discretization*, we divide the  $x$ -axis equally into  $N$  elements, with the element index  $e$  running from 1 to  $N$ . For each element  $e$ , we have  $x \in [x_{e-1}, x_e]$  and  $x_e - x_{e-1} = \ell = L/N$ . Because the two ends of the wire are clamped, we have the boundary conditions:  $\{Z, Y\}(\{0, L\}, t) = 0$ , and  $\{Z', Y'\}(\{0, L\}, t) = 0$ . To choose proper *base functions*, we note that, to preserve the physical condition of continuity of beam deflections, the nodal displacement values must be matched for any pair of neighboring elements. To obtain physically correct results that require smoothness, a second-order approximation can be used so that both the displacement and the slope of the wire at the nodal points are continuous between the neighboring elements. Consequently, for element  $e$ , at least second order or four degrees of freedom, i.e.,  $Y(x_{e-1}), Y'(x_{e-1}), Z(x_e), Z'(x_e)$ , at both ends of the element, are needed. In this setup, each node has two unknown values, and there are  $2(N-1)$  unknowns in total for the whole nanowire (excluding the two clamped ends). We then use a standard weighted-residue method in FE analysis to derive the *element equations*, where the selection of the weight functions is key. We use the Galerkin’s formulation [54–56], where the base functions are selected as the weight functions. For the nanowire system, the integrals in the original PDE can be analytically calculated, making the whole computational process extremely efficient. Then, having obtained a matrix representation of the element equations, we can *assemble* them in a proper way to derive the global equation of motion by using the fact that each node  $x_i$  ( $i \neq 0, N$ ) is shared by two elements. Finally, we use the standard second order method for integrating stochastic ODEs [57] to solve the set of initial-value problems. A detailed description of the numerical procedure, including treatment of the colored noise, is given in Appendix.

*Measure of coherence resonance.* Theoretical [36–42] and experimental [43–45] works on coherence resonance addressed excitable dynamical systems that typically generate bursting time series. In such a system, there is usually a reference or a “silent” state, e.g., a fixed point, near which a trajectory can spend long stretches of time. The trajectory can leave the reference state and return to its neighborhood in relatively short time, giving rise to a “burst.” The bursts can be due to the inherent dynamics of the system itself, or they can be excited by external perturbations or noise

through some threshold mechanism, as exemplified by the firing behavior of many types of neurons in biological systems. The bursts can occur at either relatively regular or random time intervals, for which the corresponding Fourier spectrum either contains a pronounced peak or has a broad-band feature. Coherence resonance means that noise can play the role of either improving the sharpness of the existing spectral peak, as in the former case, or inducing a pronounced spectral peak and enhancing it, as in the latter case. The idea of characterizing coherence resonance using bursting time series can be generalized. For example, for a nonexcitable system (such as our driven nanowire system), setting a proper threshold can lead to bursting-like time series.

To search for and characterize coherence resonance in the nanowire system, we use the following quantitative measure [32]:

$$\beta_T = \frac{\langle T \rangle}{\sqrt{\text{Var}(T)}}, \quad (7)$$

where  $T$  is the interval between bursts,  $\langle T \rangle$  and  $\text{Var}(T)$  are the average value and variance of  $T$ , respectively. A larger value of  $\beta_T$  indicates that the corresponding signal has a small variance, so it is more regular, and vice versa. A coherence resonance can be identified when the plot of  $\beta_T$  versus the noise amplitude  $D$  exhibits a “bell-shape” type of behavior, indicating that  $\beta_T$  can be maximized by some optimal noise amplitude.

### III. RESULTS

To demonstrate coherence resonance, we use the following experimentally feasible parameter setting [18]. The nanowire is made of silicon, its length and diameter are  $L = 3 \mu\text{m}$  and  $d = 20 \text{ nm}$ , respectively, and it is placed under room conditions:  $P = 1.0 \text{ atm}$  and  $T = 300 \text{ K}$ . The natural frequency of the wire is  $f_0 = 3.56 \sqrt{EI/(L^4 \rho A)}$  and the frequency of the ac voltage is set to be  $f = 3f_0$ . The material parameters of silicon are  $E = 169 \text{ GPa}$  and  $\rho = 2332 \text{ kg/m}^3$ . The molecular mass of the air is  $m = 5.6 \times 10^{-26} \text{ kg}$ , the dc bias voltage is  $V_{\text{dc}} = 12 \text{ V}$ , and the gate trench height is  $h = 0.2 \mu\text{m}$ . For convenience, the initial conditions for solving the initial-value problem are chosen to be

$$\begin{aligned} Z(t=0, x) &= z_0 \sin(\pi x/L), \\ v_z(t=0, x) &= v_{z0} \cos(\pi x/L), \end{aligned} \quad (8)$$

for  $x \in [0, L]$ , where  $z_0$  and  $v_{z0}$  can be adjusted. The initial position and velocity in the  $y$  direction are fixed. The wire is divided into thirteen spatial elements and the time step in the stochastic ODE solver is set to be  $10^{-4}$ . For this parameter setting, in the absence of noise, the nanowire exhibits planar motion for  $V_{\text{ac}} < V_{\text{ac}}^1 \approx 0.595 \text{ V}$ . The planar motion becomes unstable and nonplanar motion arises for  $V_{\text{ac}} > V_{\text{ac}}^1$ . As  $V_{\text{ac}}$  is increased further, a cascade of period-doubling bifurcations occurs, leading to small-scale chaotic oscillations for  $V_{\text{ac}} >$

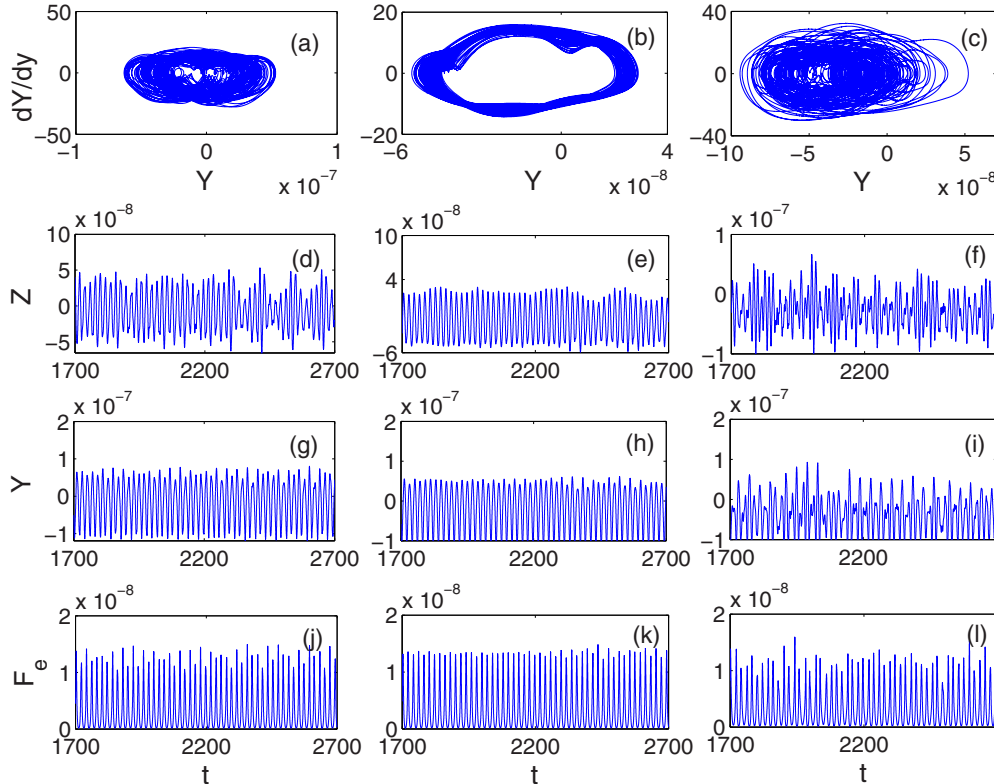


FIG. 2. (Color online) For  $V_{\text{ac}} = 6.9 \text{ V}$  (so that the nanowire system exhibits small-scale chaos) and three values of the noise amplitude:  $D = 3.5 \times 10^{-9}$ ,  $7.7 \times 10^{-9}$ , and  $2 \times 10^{-8}$ , (a)–(c) projections of the chaotic attractor in the  $(Y, dY/dt)$  plane; (d)–(f) time series of the  $z$  displacement  $Z(t)$ , (g)–(i) time series of the  $y$  displacement  $Y(t)$ , and (j)–(l) time series of the instantaneous electrical force  $F_e(t)$ , respectively. All time series are displayed for 1000 time units.

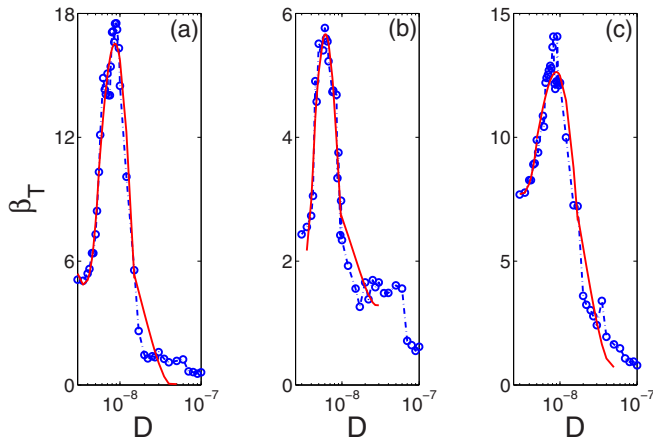


FIG. 3. (Color online) For  $V_{ac} = 6.9$  V (small-scale chaos), coherence-resonance measure  $\beta_T$  as a function of the noise amplitude  $D$ , where the time series used in (a)–(c) are  $Z(t)$ ,  $Y(t)$ , and  $F_e(t)$ , respectively. There exists an optimal value of  $D$  at which the temporal regularity of the chaotic motion is maximized. Red solid lines are POLYFIT curves.

$V_{ac}^2 \approx 6.882$  V. In this regime, there are two coexisting small chaotic attractors. For  $V_{ac} > V_{ac}^3 \approx 6.946$  V, the two small attractors merge into a large chaotic attractor, generating extensive chaos in the phase space [18].

We now present evidence that chaos in the nanowire system can be suppressed by noise through the mechanism of coherence resonance. For this purpose, we choose two values of  $V_{ac}$ , corresponding to small-scale and extensive

chaos, respectively. Figures 2(a)–2(c) show, for  $V_{ac} = 6.9$  V and three values of the noise amplitude  $D$ , phase-space plots of the chaotic attractor in the plane defined by  $Y$  and  $dY/dt$ . We observe that, for both small and large values of  $D$  [Figs. 2(a) and 2(c)], the projections of the attractors are more “space-filling,” indicating a high degree of randomness. However, for intermediate noise amplitude [Fig. 2(b)], the attractor has a more pronounced structure, indicating a significant reduction in randomness and, accordingly, much stronger regularity. Figures 2(d)–2(f) show the representative time series of the  $z$  displacement  $Z(t)$  of the nanowire for the three noise levels, respectively. Time series of the  $y$  displacement  $Y(t)$  and of the instantaneous electrical force  $F_e(t)$  are shown in Figs. 2(g)–2(i) and 2(j)–2(l), respectively. The effect of noise to regularize the chaotic motion can even be noted visually, as the time series in the middle column of Fig. 2 (for the intermediate value of  $D$ ) appear more “regular” than those for both the small and large noise cases in the left and right columns, respectively. Figures 3(a)–3(c) show the measure of coherence resonance  $\beta_T$  as a function of the noise amplitude  $D$  calculated from the time series  $Z(t)$ ,  $Y(t)$ , and  $F_e(t)$ , respectively. In all three cases,  $\beta_T$  exhibits a bell-shape type of behavior, and there exists an optimal level of noise at which the regularity of the time series can be improved significantly as compared with the case of near zero-noise amplitude, where the wire motion is nearly deterministic. Similar effects of noise to regularize chaos have been observed when the nanowire system is in the regime of extensive chaos, as shown in Figs. 4 and 5. We also find that the coherence-resonance phenomenon is robust with respect to the nature of noise. In particular, similar behavior

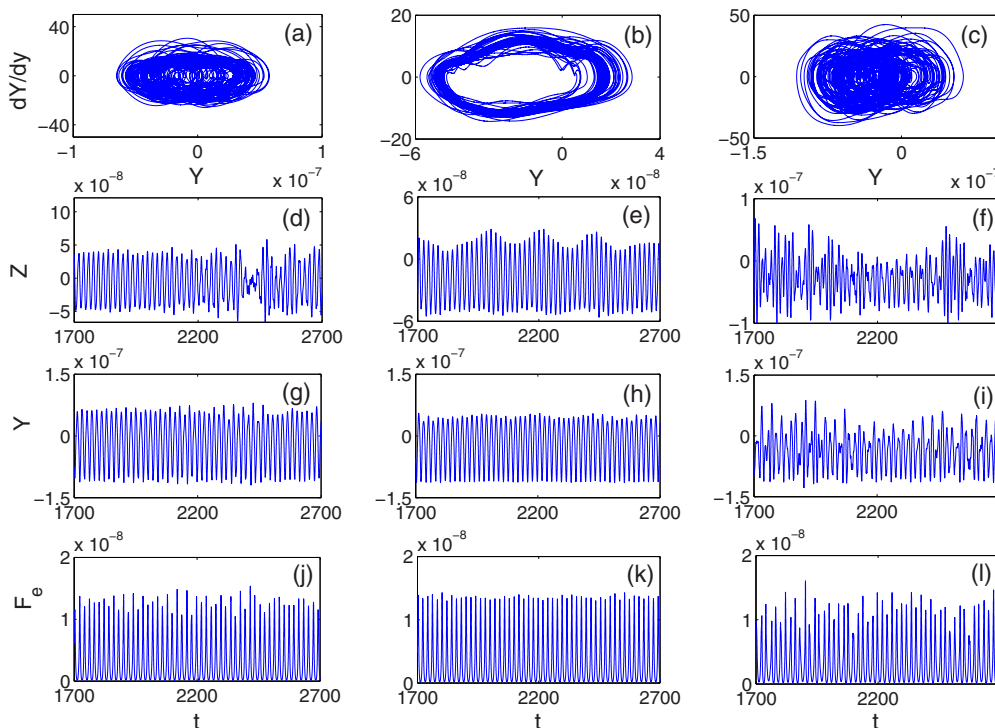


FIG. 4. (Color online) For  $V_{ac} = 6.96$  V (so that the nanowire system exhibits extensive chaos) and three values of the noise amplitude:  $D = 3.7 \times 10^{-9}$ ,  $7.7 \times 10^{-9}$ , and  $2 \times 10^{-8}$ , (a)–(c) projections of the chaotic attractor in the  $(Y, dY/dt)$  plane; (d)–(f) time series of the  $z$  displacement  $Z(t)$ , (g)–(i) time series of the  $y$  displacement  $Y(t)$ , and (j)–(l) time series of the instantaneous electrical force  $F_e(t)$ , respectively. All time series are displayed for 1000 time units.

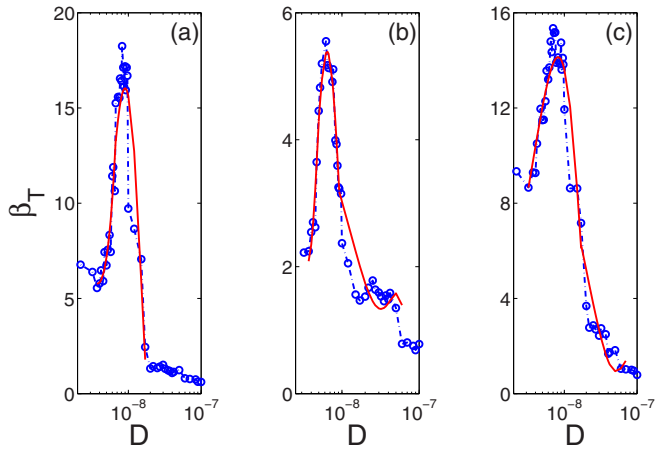


FIG. 5. (Color online) For  $V_{ac} = 6.96$  V (extensive chaos), coherence-resonance measure  $\beta_T$  as a function of the noise amplitude  $D$ , where the time series used in (a)–(c) are  $Z(t)$ ,  $Y(t)$ , and  $F_e(t)$ , respectively. There exists an optimal value of  $D$  at which the temporal regularity of the chaotic motion is maximized.

of  $\beta_T$  has been observed when the stochastic drivings in the  $y$  and  $z$  directions are independent, as exemplified in Figs. 6 and 7. Similar features of  $\beta_T$  have also been obtained for colored noise, as exemplified in Fig. 8.

Theoretically, the mechanism through which coherence resonance can occur in nonbursting nonlinear dynamical systems can be understood, as follows. In order for a resonance to occur, it is necessary to have two independent and competing time scales. At least one time scale should depend on noise. To gain insight we consider a chaotic system with a simple rotational structure so that there is a well-defined internal time scale  $\tau_{int}$ . This time scale is deterministic and it does not change

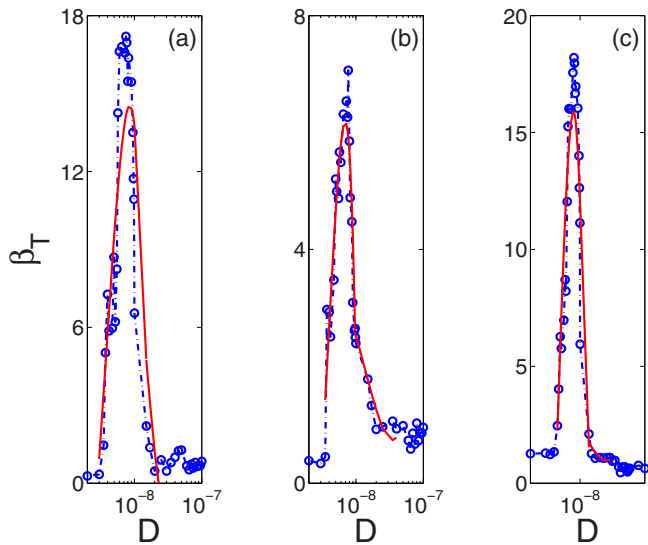


FIG. 6. (Color online) (a)–(c) For nanowire in the regime of extensive chaos ( $V_{ac} = 6.96$  V) and independent noise of identical amplitude in the  $y$  and  $z$  directions, coherence-resonance measure  $\beta_T$  as a function of the noise amplitude  $D$  for  $Z(t)$ ,  $Y(t)$ , and  $F_e(t)$ , respectively.

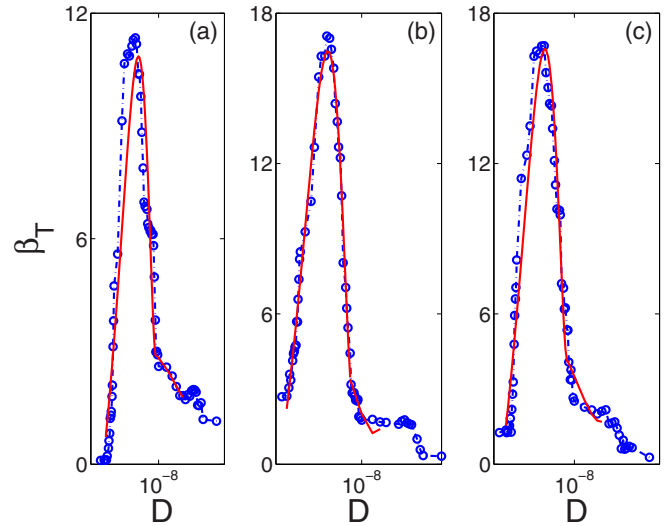


FIG. 7. (Color online) (a)–(c) For nanowire in the regime of extensive chaos ( $V_{ac} = 6.96$  V) and independent noise of different amplitude in the  $y$  and  $z$  directions, coherence-resonance measure  $\beta_T$  as a function of the noise amplitude  $D$  in the  $y$  direction (the noise amplitude in the  $z$  direction is fixed at  $D = 10^{-9}$ ) for  $Z(t)$ ,  $Y(t)$ , and  $F_e(t)$ , respectively.

with noise. Noise, however, can induce another time scale. This can be seen by realizing that for a chaotic attractor, which is bounded in the phase space, in general there exists a *reference* state, such as that due to the harmonic oscillator embedded in the differential equations in the chaotic Rössler system [58]. Noise can cause a trajectory initiated in the reference state to wander away from it. Since the system is bounded, at a later time the trajectory will come back to the reference state. On average, this process defines a time scale, which is the stochastic first-passage time with respect to the reference state. This is an “external” time scale induced by noise, which

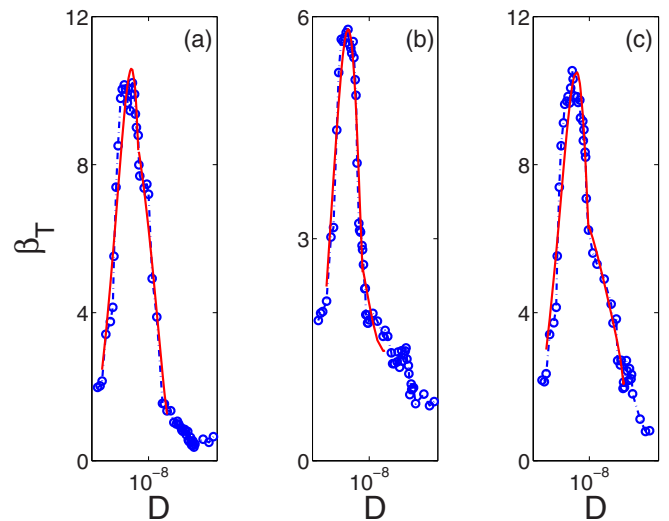


FIG. 8. (Color online) (a)–(c) For  $V_{ac} = 6.96$  V (nanowire in the regime of extensive chaos) and colored noise of amplitude  $D$ , coherence-resonance measure  $\beta_T$  as a function of  $D$  for  $Z(t)$ ,  $Y(t)$ , and  $F_e(t)$ , respectively.

depends on the noise amplitude  $D$ . We write it as  $\tau_{\text{ext}}(D)$ . As the noise is strengthened, we expect to see a resonance at the optimal noise level  $D^*$ , where  $\tau_{\text{ext}}(D^*) = \tau_{\text{int}}$ .

The above heuristic argument can be made more quantitative. In particular, the existence of an external stochastic time scale  $\tau_{\text{ext}}$  and how it varies with noise can be studied by considering the following simple one-dimensional model with a reference state, under the influence of noise:  $dx/dt = [-\lambda + h(t)]x + D\xi(t)$ , where  $e^\lambda$  is the largest eigenvalue of the reference state  $x = 0$ ,  $h(t)$  is a zero-mean process (either random or chaotic) that models the finite-time fluctuations in the stability of the reference state, and  $D\xi(t)$  is the external noise. The time series  $x(t)$  is therefore a realization of some stochastic process  $X(t)$ , and its probability distribution function  $P(x, t)$  obeys the Fokker-Planck equation,

$$\frac{\partial P}{\partial t} = -\frac{\partial}{\partial x} \left[ \left( -\lambda x + \frac{1}{2} \eta x \right) P \right] + \frac{1}{2} \frac{\partial^2}{\partial x^2} [(\eta x^2 + D)P], \quad (9)$$

where  $\eta$  is the amplitude of  $h(t)$ . To compute the first passage time, assume there is an absorbing boundary at  $x = a$ . The boundedness of the system implies that there must be a reflecting boundary at  $x = b$ . With these boundary conditions, the Fokker-Planck equation can be solved to yield the following expression for the first-passage time [57]:

$$\langle T \rangle = 2 \int_{x_0}^a dy (\eta y^2 + D)^{\lambda/\eta - 1/2} \int_b^y (\eta z^2 + D)^{-1/2 - \lambda/\eta} dz, \quad (10)$$

where  $x_0$  is the initial value of  $x(t)$  and  $\tau_{\text{ext}} \sim \langle T \rangle$ . The general feature is that the external frequency  $\omega_{\text{ext}} \sim 1/\langle T \rangle$  depends on the noise amplitude. Since the internal frequency  $\omega_{\text{int}} \sim 1/\tau_{\text{int}}$  is approximately constant, generically the  $\omega_{\text{ext}}(D)$  curve can intersect with  $\omega_{\text{int}}$  at some optimal noise amplitude  $D^*$ , leading to the time-scale match required for coherence resonance. The optimal noise level  $D^*$  depends on the details of the system and cannot be predicted by the heuristic theory.

For a more general nonlinear system such as our driven nanowire system, the internal time scale  $\tau_{\text{int}}$  can be regarded as arising from the recurrence of the flow. For instance, one can imagine a Poincaré surface of section and observe the average time interval between successive piercings through the section. Coherence resonance can occur when this deterministic time matches the first-passage time induced by noise.

#### IV. CONCLUSION

We have uncovered the phenomenon of coherence resonance in electrically driven nanowire systems and exploited its use in regularizing chaos. Due to the strongly nonlinear nature in the dynamics of the nanowire, there are wide parameter regimes in which the wire exhibits chaotic oscillations. It is difficult to apply the conventional methods of chaos control, because of (a) the extremely high-dimensional phase space of the nanowire system, and (b) the challenge in monitoring the detailed motion of the wire to gather information necessary for implementing the control. Our results indicate that chaos can be suppressed by noise to yield much more regular oscillations and consequently much more regular output signals in device

applications. Our finding of coherence resonance in nanoscale systems, besides its fundamental importance, has the practical advantage of providing a feasible way to regularize chaos. Especially, one can imagine placing a chaotic nanowire system in an environment where temperature and, consequently, the amplitude of noise, can be adjusted.

#### ACKNOWLEDGMENTS

Y. Do was supported by Basic Science Research Program through the National Research Foundation of Korea(NRF) funded by the Ministry of Education, Science and Technology(MEST) (NRF-2013R1A1A2010067). YCL and JSC were supported by the NSF (USA) under Grant No. EPDT-1101797. P. Hessari and C. W. Park were supported by NRF grant funded by MEST (No. 2012R1A2A2A01046099), and a grant from the Priority Research Centers Program through NRF funded by MEST (2012-0005856). GW Lee was supported by the Korea Meteorological Administration Research and Development Program under Grant CATER 2013-2040.

#### APPENDIX

For completeness, we briefly describe the method of solving PDEs of electrically driven nanowire systems [19], which we combine with the method for solving ODEs subject to colored noise [59]. We begin by writing Eq. (1) as

$$\begin{aligned} -\ddot{Z} + c_1 \dot{Z} + c_2 Z'''' + c_3 I_0 Z'' &= F_e(Z) + \eta, \\ -\ddot{Y} + c_1 \dot{Y} + c_2 Y'''' + c_3 I_0 Y'' &= \eta, \end{aligned} \quad (A1)$$

$$\dot{\eta} = -\lambda \eta + \lambda g_w,$$

where  $I_0 = \int_0^L (Y_x^2 + Z_x^2) dx$ , constants  $c_1$ ,  $c_2$ , and  $c_3$  are given by

$$c_1 = -\frac{\pi P d}{4\rho A v_T}, \quad c_2 = -\frac{EI}{\rho A}, \quad c_3 = \frac{E}{2\rho L},$$

the electrical force  $F_e(Z)$  is normalized by  $1/(\rho A)$ , and  $g_w$  is a Gaussian random process of zero mean and unit variance. Colored noise is modeled by an exponentially correlated stochastic process, the Ornstein-Uhlenbeck process, with the following properties:

$$\begin{aligned} \langle \eta(t) \rangle &= 0, \\ \langle \eta(t) \eta(s) \rangle &= D\lambda \exp(-\lambda|t - s|), \end{aligned} \quad (A2)$$

where  $\lambda^{-1}$  is the correlation time of the process. We divide the  $x$ -range of the nanowire into  $N$  equal element:  $e = 1, \dots, N$ . For each element  $e$ , we have  $x \in [x_{e-1}, x_e]$  and  $x_e - x_{e-1} = \ell = L/N$ . The boundary conditions are  $\{Y, Z\}(\{0, L\}, t) = 0$ , and  $\{Y', Z'\}(\{0, L\}, t) = 0$ . For an element  $e$ , we have four degrees of freedom:  $Z(x_{e-1}, t)$ ,  $Z'(x_{e-1}, t)$ ,  $Z(x_e, t)$ , and  $Z'(x_e, t)$ . We use the interpolation approximation model

$$Z^e(x, t) = \sum_{i=1}^4 \phi_i(x) q_i^e(t), \quad (A3)$$

where  $\phi_i(x)$ 's are basis functions and  $q^e(t) = [Z(x_{e-1}, t), Z'(x_{e-1}, t), Z(x_e, t), Z'(x_e, t)]^T$  is the unknown vector for element  $e$ . Letting  $\bar{x} = x - x_{e-1}$  and  $s = \bar{x}/\ell$ , we

have  $\bar{x} \in [0, \ell]$ ,  $s \in [0, 1]$ . We express the displacement in terms of the third-order polynomials:

$$Z^e(\bar{x}) = [1 \ \bar{x} \ \bar{x}^2 \ \bar{x}^3] \cdot [a_0^e \ a_1^e \ a_2^e \ a_3^e]^T = X \cdot A^e,$$

so  $Z^{e'}(\bar{x}) = X' \cdot A^e$ . Setting  $\bar{x} = 0, \ell$ , for  $Z^e(\bar{x})$  and  $Z^{e'}(\bar{x})$ , we have

$$q^e = \begin{bmatrix} 1 & 0 & 0 & 0 \\ 0 & 1 & 0 & 0 \\ 1 & \ell & \ell^2 & \ell^3 \\ 0 & 1 & 2\ell & 3\ell^2 \end{bmatrix} A^e = B A^e.$$

The displacement  $Z^e(\bar{x})$  can be written as

$$Z^e(\bar{x}) = X A^e = X B^{-1} q^e.$$

Comparing the above equation with Eq. (A3), we get the following basis function:

$$\phi = [1 - 3s^2 + 2s^3, \ell s(1 - 2s + s^2), s^2(3 - 2s), \ell s^2(s - 1)]^T,$$

which allows us to implement the Galerkin method [54–56],

$$\int_{x_{e-1}}^{x_e} (-\ddot{Z} + c_1 \dot{Z} + c_2 Z'''' + c_3 I_0 Z'' - F_e - \eta) \phi_i(x) dx = 0,$$

for  $i = 1, 2, 3, 4$ . Integrating by parts, we have

$$\begin{aligned} \int_{x_{e-1}}^{x_e} \ddot{Z} \phi_i(x) dx &= c_2 \int_{x_{e-1}}^{x_e} Z'' \phi_i''(x) + c_2 (Z''' \phi_i - Z'' \phi_i') \Big|_{x_{e-1}}^{x_e} \\ &\quad + c_3 I_0 \int_{x_{e-1}}^{x_e} Z'' \phi_i(x) dx \\ &\quad + c_1 \int_{x_{e-1}}^{x_e} \dot{Z} \phi_i(x) dx - \int_{x_{e-1}}^{x_e} F_e \phi_i(x) dx \\ &\quad - \int_{x_{e-1}}^{x_e} \eta \phi_i(x) dx. \end{aligned}$$

Substituting Eq. (A3) into the above, we arrive at

$$\begin{aligned} M_1^e \ddot{q}^e &= c_2 M_2^e q^e + c_3 I_0 M_3^e q^e \\ &\quad + c_1 M_4^e \dot{q}^e + f_{\text{gen}}^e - f_{\text{ext}}^e - \eta F_n, \end{aligned} \quad (\text{A4})$$

where

$$M_1^e(i, j) = \int_{x_{e-1}}^{x_e} \phi_i(x) \phi_j(x) dx,$$

$$M_2^e(i, j) = \int_{x_{e-1}}^{x_e} \phi_i''(x) \phi_j''(x) dx,$$

$$M_3^e(i, j) = \int_{x_{e-1}}^{x_e} \phi_i''(x) \phi_j(x) dx,$$

$$M_4^e(i, j) = \int_{x_{e-1}}^{x_e} \phi_i'(x) \phi_j'(x) dx,$$

$$F_n = \begin{bmatrix} \ell/2 \\ \ell^2/12 \\ \ell/2 \\ -\ell^2/12 \end{bmatrix},$$

$$\begin{aligned} f_{\text{gen}}^e &= c_2 (Z''' \phi_i - Z'' \phi_i') \Big|_{x_{e-1}}^{x_e} \\ &= [-Z'''(x_{e-1}), -Z''(x_{e-1}), Z'''(x_e), -Z''(x_e)]^T. \end{aligned}$$

For the electric force, we use the linear approximation:

$$F_e(s, t) = (1 - s)f_1(t) + sf_2(t),$$

where  $f_1$  and  $f_2$  are the forces exerted on the two ends of the element. We have

$$\begin{aligned} F_e^e &= \int_{x_{e-1}}^{x_e} [(1 - s)F_e(x_{e-1}) + sF_e(x_e)] \phi(x) dx \\ &= \begin{bmatrix} \ell(7f_{e-1} + 3f_e)/20 \\ \ell^2(3f_{e-1} + 2f_e)/60 \\ \ell(3f_{e-1} + 7f_e)/20 \\ \ell^2(-2f_{e-1} - 3f_e)/60 \end{bmatrix}. \end{aligned}$$

We can now assemble the global matrices and force vectors,

$$\begin{aligned} M_i^{\text{all}} &= (\oplus_{k=1}^{[N/2]} M_k^e) \oplus \mathbf{0}_{1+(-1)^N} + \mathbf{0}_2 \\ &\quad + \oplus (\oplus_{k=1}^{[N/2]} M_k^e) \oplus \mathbf{0}_{1-(-1)^N}, \end{aligned}$$

for  $i = 1, 2, 3$ , where  $M_i^{\text{all}}$  is a  $2(N - 1) \times 2(N - 1)$  global assembled matrix for  $M_i^e$  and  $\mathbf{0}_j$  is a  $j \times j$  zero matrix. The general and external force vectors, as well as the vector  $F_n$ , can be assembled as

$$f_{\text{gen}}^{\text{all}} = [-Z'''(0), -Z''(0), 0, \dots, 0, -Z'''(L), -Z''(L)]^T,$$

$$f_{\text{ext}}^{\text{all}} = \begin{bmatrix} \frac{\ell(7f_0 + 3f_1)/20}{\ell^2(3f_0 + 2f_1)/60} \\ \frac{\ell(3f_0 + 14f_1 + 3f_2)/20}{\ell^2(-f_0 + f_2)/30} \\ \vdots \\ \frac{\ell(3f_{N-2} + 14f_{N-1} + 3f_N)/20}{\ell^2(-f_{N-2} + f_N)/30} \\ \frac{\ell(3f_{N-1} + 7f_N)/20}{\ell^2(-2f_{N-1} - 3f_N)/60} \end{bmatrix},$$

and

$$F_n^{\text{all}} = \begin{bmatrix} \ell/2 \\ \ell^2/12 \\ \ell \\ 0 \\ \vdots \\ \ell \\ 0 \\ \ell/2 \\ -\ell^2/12 \end{bmatrix}.$$

By imposing boundary conditions, we have  $2(N - 1)$  unknowns:

$$\mathbf{Z} = [Z_1, Z'_1, Z_2, Z'_2, \dots, Z_{N-1}, Z'_{N-1}]^T.$$

We remove the first and last two components of vectors  $f_{\text{ext}}^{\text{all}}$  and  $f_{\text{gen}}^{\text{all}}$ . Similarly, we remove the first and last two columns and rows of matrices  $M_i^{\text{all}}$ ,  $i = 1, 2, 3$ . After assembly and modification, Eq. (A4) becomes

$$\begin{aligned} \ddot{\mathbf{Y}} &= c_1 \dot{\mathbf{Y}} + (c_2 M_1^{-1} M_2 + c_3 I_0 M_1^{-1} M_3) \mathbf{Y} - M^{-1} \eta F_n^{\text{all}}, \\ \ddot{\mathbf{Z}} &= c_1 \dot{\mathbf{Z}} + (c_2 M_1^{-1} M_2 + c_3 I_0 M_1^{-1} M_3) \mathbf{Z} \\ &\quad - M_1^{-1} F_{\text{ext}} - M^{-1} \eta F_n^{\text{all}}. \end{aligned} \quad (\text{A5})$$



By substituting Eq. (A3) in  $I_0$  for  $Z$ , we have

$$I_0^Z = \sum_{i,j=1}^4 M_4(i,j) \sum_{e=1}^N q_i^e q_j^e.$$

Setting  $Y^e(x,t) = \sum_{i=1}^4 \phi_i(x) p_i^e(t)$ , we obtain

$$I_0 = \sum_{i,j=1}^4 M_4(i,j) \sum_{e=1}^N (q_i^e q_j^e + p_i^e p_j^e).$$

We finally arrive at the following system of stochastic ODEs subject to colored noise:

$$\frac{d}{dt} \begin{bmatrix} \mathbf{Y} \\ \mathbf{Y}^t \\ \mathbf{Z} \\ \mathbf{Z}^t \\ \eta \end{bmatrix} = \begin{bmatrix} \mathbf{Y}^t \\ c_1 \mathbf{Y}^t + (c_2 M_1^{-1} M_2 + c_3 I_0 M_1^{-1} M_3) \mathbf{Y} - M^{-1} \eta F_n^{\text{all}} \\ \mathbf{Z}^t \\ c_1 \mathbf{Z}^t + (c_2 M_1^{-1} M_2 + c_3 I_0 M_1^{-1} M_3) \mathbf{Z} - M_1^{-1} F_{\text{ext}} - M^{-1} \eta F_n^{\text{all}} - \lambda \eta + \lambda g_w \end{bmatrix}, \quad (\text{A6})$$

with the initial condition

$$\begin{bmatrix} \mathbf{Y}(0) \\ \mathbf{Y}^t(0) \\ \mathbf{Z}(0) \\ \mathbf{Z}^t(0) \\ \eta(0) \end{bmatrix} = \begin{bmatrix} \mathbf{Y}_0 \\ \mathbf{Y}_0^t \\ \mathbf{Z}_0 \\ \mathbf{Z}_0^t \\ \eta_0 \end{bmatrix}.$$

To solve the above ODE system numerically, we use the algorithm for integrating stochastic differential equations under colored noise, developed by Fox *et al.* [59]. First, we rewrite the ODE system as

$$\dot{\mathbf{X}} = \mathbf{F}(\mathbf{X}) + \eta, \quad \dot{\eta} = -\lambda \eta + \lambda g_w.$$

The subsequent steps are to set  $E = e^{-\lambda \Delta t}$ , to let  $m, n, a$  and  $b$  be random variables, and to integrate the following stochastic differential-equation system using the standard second-order method [57]:

$$\begin{aligned} \eta &= [-2D\lambda \ln(m)]^{1/2} \cos(2\pi n), & p &= \mathbf{F}(\mathbf{X}) + \eta, & \mathbf{X}|_{t+\Delta t} &= \mathbf{X} + p \Delta t, \\ h &= [-2D\lambda(1 - E^2) \ln(a)]^{1/2} \cos(2\pi b), & \eta|_{t+\Delta t} &= \eta E + h. \end{aligned}$$

- 
- [1] D. Rugar, R. Budakian, H. Mamin, and B. Chui, *Nature (London)* **430**, 329 (2004).
- [2] Y. T. Yang, C. Callegari, X. L. Feng, K. L. Ekinici, and M. L. Roukes, *Nano Lett.* **6**, 583 (2006).
- [3] P. Gammel, G. Fischer, and J. Bouchaud, *Bell Labs Tech.* **10**, 29 (2005).
- [4] M. Patra, G. Schwarz, and E. Schöll, *Phys. Rev. B* **57**, 1824 (1998).
- [5] Y. Bomze, R. Hey, H. T. Grahn, and S. W. Teitworth, *Phys. Rev. Lett.* **109**, 026801 (2012).
- [6] P. Kim and C. M. Lieber, *Science* **286**, 2148 (1999).
- [7] T. Rueckes, K. Kim, E. Joselevich, G. Y. Tseng, C.-L. Cheung, and C. M. Lieber, *Science* **289**, 94 (2000).
- [8] M. Dequesnes, S. V. Rotkin, and N. R. Aluru, *Nanotechnol.* **13**, 120 (2002).
- [9] S. N. Cha, J. E. Jang, Y. Choi, G. A. J. Amaratunga, D.-J. Kang, D. G. Hasko, J. E. Jung, and J. M. Kim, *Appl. Phys. Lett.* **86**, 083105 (2005).
- [10] J. S. Aldridge and A. N. Cleland, *Phys. Rev. Lett.* **94**, 156403 (2005).
- [11] E. Buks and B. Yurke, *Phys. Rev. E* **74**, 046619 (2006).
- [12] I. Kozinsky, H. W. C. Postma, I. Bargatin, and M. L. Roukes, *Appl. Phys. Lett.* **88**, 253101 (2006).
- [13] I. Kozinsky, H. W. C. Postma, O. Kogan, A. Husain, and M. L. Roukes, *Phys. Rev. Lett.* **99**, 207201 (2007).
- [14] W. G. Conley, A. Raman, C. M. Krousgrill, and S. Mohammadi, *Nano Lett.* **8**, 1590 (2008).
- [15] S. Shim, M. Imboden, and P. Mohanty, *Science* **316**, 95 (2007).
- [16] D. N. Guerra, T. Dunn, and P. Mohanty, *Nano Lett.* **9**, 3096 (2009).
- [17] T. Dunn, D. N. Guerra, and P. Mohanty, *Eur. Phys. J. B* **69**, 5 (2009).
- [18] Q.-F. Chen, L. Huang, Y.-C. Lai, C. Grebogi, and D. Dietz, *Nano Lett.* **10**, 406 (2010).
- [19] X. Ni, L. Ying, Y.-C. Lai, Y.-H. Do, and C. Grebogi, *Phys. Rev. E* **87**, 052911 (2013).
- [20] H. W. C. Postma, I. Kozinsky, A. Husain, and M. L. Roukes, *Appl. Phys. Lett.* **86**, 223105 (2005).
- [21] R. He, X. L. Feng, M. L. Roukes, and P. Yang, *Nano Lett.* **8**, 1756 (2008).
- [22] W. Y. Fung, E. N. Dattoli, and W. Lu, *Appl. Phys. Lett.* **94**, 203104 (2009).
- [23] E. Ott, C. Grebogi, and J. A. Yorke, *Phys. Rev. Lett.* **64**, 1196 (1990).
- [24] S. Boccaletti, C. Grebogi, Y.-C. Lai, H. Mancini, and D. Maza, *Phys. Rep.* **329**, 103 (2000).

- [25] R. Benzi, A. Suter, and A. Vulpiani, *J. Phys. A* **14**, L453 (1981).
- [26] R. Benzi, G. Parisi, A. Suter, and A. Vulpiani, *Tellus* **34**, 10 (1982).
- [27] B. McNamara and K. Wiesenfeld, *Phys. Rev. A* **39**, 4854 (1989).
- [28] F. Moss, D. Pierson, and D. O’Gorman, *Int. J. Bif. Chaos* **4**, 1383 (1994).
- [29] P. C. Gailey, A. Neiman, J. J. Collins, and F. Moss, *Phys. Rev. Lett.* **79**, 4701 (1997).
- [30] L. Gammaitoni, P. Hänggi, P. Jung, and F. Marchesoni, *Rev. Mod. Phys.* **70**, 223 (1998).
- [31] D. Sigei and W. Horsthemke, *J. Stat. Phys.* **54**, 1217 (1989).
- [32] A. S. Pikovsky and J. Kurths, *Phys. Rev. Lett.* **78**, 775 (1997).
- [33] Z. Liu and Y.-C. Lai, *Phys. Rev. Lett.* **86**, 4737 (2001).
- [34] Y.-C. Lai and Z. Liu, *Phys. Rev. E* **64**, 066202 (2001).
- [35] Gang Hu, T. Ditzinger, C. Z. Ning, and H. Haken, *Phys. Rev. Lett.* **71**, 807 (1993).
- [36] A. Neiman, P. I. Saparin, and L. Stone, *Phys. Rev. E* **56**, 270 (1997).
- [37] T. Ohira and Y. Sato, *Phys. Rev. Lett.* **82**, 2811 (1999).
- [38] A. Neiman, L. Schimansky-Geier, A. Cornell-Bell, and F. Moss, *Phys. Rev. Lett.* **83**, 4896 (1999).
- [39] J. R. Pradines, G. V. Osipov, and J. J. Collins, *Phys. Rev. E* **60**, 6407 (1999).
- [40] B. Lindner and L. Schimansky-Geier, *Phys. Rev. E* **60**, 7270 (1999).
- [41] B. Lindner and L. Schimansky-Geier, *Phys. Rev. E* **61**, 6103 (2000).
- [42] Y. Yu, W. Wang, J. Wang, and F. Liu, *Phys. Rev. E* **63**, 021907 (2001).
- [43] D. E. Postnov, S. K. Han, T. G. Yim, and O. V. Sosnovtseva, *Phys. Rev. E* **59**, R3791 (1999).
- [44] S. K. Han, T. G. Yim, D. E. Postnov, and O. V. Sosnovtseva, *Phys. Rev. Lett.* **83**, 1771 (1999).
- [45] G. Giacomelli, M. Giudici, S. Balle, and J. R. Tredicce, *Phys. Rev. Lett.* **84**, 3298 (2000).
- [46] C. Palenzuela, R. Toral, and C. R. Mirasso, *Europhys. Lett.* **56**, 347 (2001).
- [47] O. Calvo, C. R. Mirasso, and R. Toral, *Electron. Lett.* **37**, 1062 (2001).
- [48] A. G. Balanov, N. B. Janson, and P. V. E. McClintock, *Fluc. Noise Lett.* **3**, L113 (2003).
- [49] C. Y. Lee, W. Choi, J.-H. Han, and M. S. Strano, *Science* **329**, 1320 (2010).
- [50] J. Escorcia-Garcia, V. Agarwal, and P. Parmanada, *Appl. Phys. Lett.* **94**, 133103 (2009).
- [51] J. Hizanidis, A. Balanov, A. Amann, and E. Schöll, *Appl. Phys. Lett.* **96**, 244104 (2006).
- [52] K. L. Ekinici, Y. T. Yang, X. M. Huang, and M. L. Roukes, *Appl. Phys. Lett.* **81**, 2253 (2002).
- [53] Y. Wang, Y.-C. Lai, and Z. Zheng, *Phys. Rev. E* **79**, 056210 (2010).
- [54] C. S. Desai and T. Kundu, *Introductory Finite Element Method*, 1st ed. (CRC Press, Boca Raton, 2001).
- [55] G. E. Karniadakis and S. Sherwin, *Spectral Element Methods for Computational Fluid Dynamics*, 2nd ed. (Oxford University Press, Oxford UK, 2005).
- [56] J. N. Reddy, *An Introduction to Finite Element Method*, 3rd ed. (McGraw-Hill, New York, 2006).
- [57] C. W. Gardiner, *Handbook of Stochastic Methods*, 2nd ed. (Springer, New York, 1985).
- [58] O. E. Rössler, *Phys. Lett. A* **57**, 397 (1976).
- [59] R. F. Fox, I. R. Gatland, R. Roy, and G. Vemuri, *Phys. Rev. A* **38**, 5938 (1988).